MRS Advances © 2018 Materials Research Society
DOI: 10.1557/adv.2018.656

The Effects of Dynamic Transformation on the Formation of Pt-M (M = Ni, Fe) Nanocrystals

Yiliang Luan[1], Can Li[1], Bo Zhao[2], Amar Kumbhar[3], Jun Zhang[4], Jiye Fang[1,*]

1. Department of Chemistry, State University of New York at Binghamton, Binghamton, NY, USA

2. College of Arts & Sciences Microscopy, Texas Tech University, Lubbock, TX, USA

3. Chapel Hill Analytical and Nanofabrication Laboratory, University of North Carolina at Chapel Hill, Chapel Hill, NC, USA

4. College of Chemical Engineering, China University of Petroleum (East China), Shandong, China

ABSTRACT

In the synthesis of metallic nanocrystals (NCs) using a high-temperature colloidal approach, the competition between deposition and diffusion of "free atom (or clusters)" plays an important role as it can direct the morphology of NCs during their evolution. This competition is closely associated with some dynamic conditions such as heat and mass transfer. Stirring speed and ramp rate of heating are two factors that greatly impact the heat and mass transfer processes and consequently determine the morphology of the products but rarely discussed in most synthetic protocols. Herein, we study the syntheses of Pt-M (M = Ni, Fe) NCs as model reactions, showing that a low stirring speed and high ramp rate of heating result in ununiform pod-like NCs, whereas the inverse conditions promote NCs in a uniform shape. This observation can be plausibly explained using a competition mechanism between the deposition and diffusion of the newly reduced atoms during a stage of the NC's growth.

INTRODUCTION

Nanomaterials possess extensive applications[1-4] due to their unique properties compared with their bulk counterparts. High-temperature colloidal synthesis approach has been widely used in the preparation of NCs including metals[5-8], alloys[8-11], semiconductors[12, 13] and oxides[14-16], as it can produce size- and shape-controlled nano-architectures. It is also one of the insightful strategies to produce NCs with exclusive facets in order to correlate a collective property such as the reaction activity or selectivity with a specific lattice plane[8, 17]. Compared with other wet-chemical approaches such as the hydrothermal method, the high-temperature colloidal synthesis contains more variable factors that govern the formation of NCs and tune their shape through both the kinetic and thermodynamic controls. As an advantage, the growth of the particle products could be precisely controlled if these processing factors are successfully identified and controlled. For example, a competition between the deposition and diffusion of the "free atoms (or clusters)" released from the precursors during the growth of an NC[18] could steer the shape evolution of the NC and involve some in-depth mechanistic insights to uncover.

A typical high-temperature colloidal synthesis set-up is illustrated in Figure 1. The system connects to a Schlenk line in order to remove the moisture and residue of the air under vacuum and to provide an inert atmosphere for reaction. A magnetic stirring in the reaction flask (not shown) helps accelerate the mass and heat transfer. In our system, a non-polar organic solvent is chosen as the high-temperature reaction medium to facilitate the formation of the NCs in the presence of selected capping ligands with an argon stream. Since the mass and heat transfer, which is closely associated with some intrinsic features of the reaction mixture such as the viscosity, determines the NC's morphology evolution, the stirring speed and ramp rate of heating are identified as two of the significant factors that could tune it and consequently steer the reaction direction through an intervention of the competition between the deposition and diffusion of the "free atoms (or clusters)" in the synthetic process. In order to investigate these factors, we exploited their correlation to the morphologies of Pt-M (M = Ni, Fe) NCs as products of model syntheses when other experimental parameters were preserved.

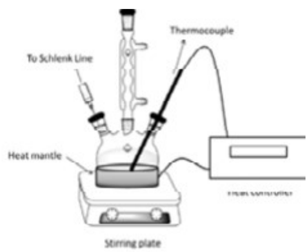

Figure 1. A typical set-up of colloidal synthesis.

EXPERIMENTAL

The syntheses of Pt-Ni octahedral NCs, cuboid NCs, and Pt-Fe cuboid NCs were carried out using a protocol established previously[9, 19].

In a typical synthesis of Pt-Ni octahedral NCs, 20.0 mg of platinum acetylacetonate ($Pt(acac)_2$), 9.5 mg of nickel chloride hexahydrate ($NiCl_2 \cdot 6H_2O$), 7.0 mL of oleylamine (OAm) and 3.0 mL of oleic acid (OA) were loaded in a three-neck flask. The mixture was heated to 90 °C under vacuum and kept for 60 min to remove the absorbed moisture and air. The stirring speed was set to 600 rpm throughout the whole synthetic procedure. The temperature was then raised to 155 °C within 5 min, during which 50.0 mg of tungsten hexacarbonyl ($W(CO)_6$) was added to the system in an argon atmosphere at 130 °C. The mixture was maintained at 155 °C for 1 min in a dark-brown color, and subsequently heated to 230 °C in a ramp rate of heating at 5 °C/min using a programed-temperature controller. The system remained at 230 °C for 40 min to allow a sufficient crystal growth before the reaction was ceased by promptly cooling to room temperature using a water bath.

The same experimental conditions were applied to the synthesis of Pt-Ni polyhedral NCs, except for 15 °C/min as the ramp rate of heating. In the case of Pt-Ni pod-like NCs synthesis, the Pt-Ni octahedral protocol was utilized except for a different stirring speed (200 rpm) and ramp rate of heating (15 °C/min).

To synthesize Pt-Ni cuboid NCs, 20.0 mg of $Pt(acac)_2$, 8.0 mL of OAm and 2.0 mL of OA were loaded in a three-neck flask. The stirring speed was set to 600 rpm through the whole protocol. After the same degassing procedure stated above was followed, the mixture was heated to 155 °C within 5 min and 50.0 mg $W(CO)_6$ was added at 130 °C in an argon atmosphere. A stock solution of Ni-precursors (0.1 M, 0.4 mL), which was pre-prepared by dissolving $NiCl_2 \cdot 6H_2O$ into a mixture of solvents containing OAm and OA with a volume ratio of 1:1, was introduced using an injection pump within 15 min while the system was steadily heated to 200 °C. The temperature was further elevated to 240 °C and maintained for an additional 15 min before the crystal growth was ceased by rapidly cooling to room temperature using a water bath. The same procedure except for a 200 rpm of stirring speed was utilized to synthesize the Pt-Ni pod-like NCs.

The synthetic procedure of Pt-Ni octahedral NCs was also applied to the preparation of Pt-Fe nanocubes when the $NiCl_2 \cdot 6H_2O$ was replaced by 10.0 mg of $FeCl_2 \cdot 4H_2O$ in the abovementioned recipe. The Pt-Fe pod-like NCs was produced by setting the stirring speed and ramp rate of heating to 200 rpm and 15 °C/min, respectively, with all the other conditions same to those in the synthesis of Pt-Fe nano-cuboid NCs.

RESULTS AND DISCUSSION

The TEM images of Pt-Ni NCs evolved by different stirring speed and heating ramp conditions are shown in Table 1 and Figure 2. When a low stirring speed (200 rpm) and high ramp rate of heating (15°C/min) were adopted, pod-like NCs with branches were produced, but the NC's shape was not uniform (Figure 2a). The NC's shape could be improved (more uniform without any branch, Figure 2b) in the case when the stirring speed was increased to 600 rpm with a preservation of the same ramp rate of heating. Consequently, the resultant NCs shifted to polyhedron-like morphology from the pod-like one at the high stirring speed rate. Alternatively, a decrease in the ramp rate of heating (5 °C/min) with a combination of high stirring speed (600 rpm) yielded dominant octahedral Pt-Ni NCs (Figure 2c).

Table 1 Morphologies Evolution Depending on the Synthetic Conditions

Stirring speed & ramp rate of heating	Morphology of Pt-Ni NCs
200 rpm & 15°C/min	Pod
600 rpm & 15°C/min	Polyhedra
600 rpm & 5°C/min	Octahedra

The shape-controlled synthetic mechanism has been intensively discussed before[8, 18]. However, the impact of stirring speed and ramp rate of heating on the product (NC) development is still remained to be uncovered. Intrinsically, the stirring speed and ramp rate of heating are closely related to the mass and heat transfer processes, which affect some dynamic processes including the deposition and diffusion in the NC's growth stage. A simple model of such a competition between the deposition and diffusion of newly reduced atoms[18] is proposed in Scheme 1 and depicts the formation mechanism of different products by tuning the stirring speed and ramp rate of heating. As shown in Scheme 1, a newly reduced atom (free atom) could proceed via two pathways in the growth process. It first deposits on an existing crystal facet, and upon the deposition, there could be two following routes for the ad-atom to go: staying where it deposited or diffusing along the crystal plane to a thermodynamically stable site. These options could be controlled by a competitive evolution between deposition and diffusion. If the deposition rate was much faster than that of the diffusion, the surface diffusion could be ignored and the deposited atom would locally accumulate to form the branches on the seed in the pod-like products. If the deposition rate was much slower than that of the diffusion, the deposited atom would migrate along the crystal plane to a low-surface-energy site and produce octahedral NCs synergistically assisted by other established experimental conditions that are not discussed here. If both rates were comparable, meaning that the diffusion was not fast enough to release the accumulated atoms brought by the deposition, it would produce the NCs with some polyhedral shapes.

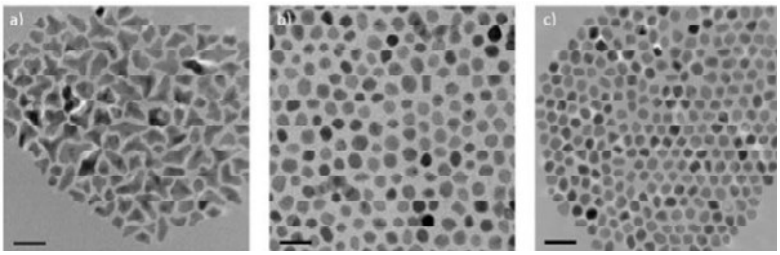

Figure 2. TEM images Pt-Ni octahedral synthesis products: (a) pod-like NCs (200 rpm, 15 °C/min), (b) polyhedron-like NCs (600 rpm, 15 °C/min) and (c) octahedral NCs (600 rpm, 5 °C/min). Each scale bar represents 30 nm.

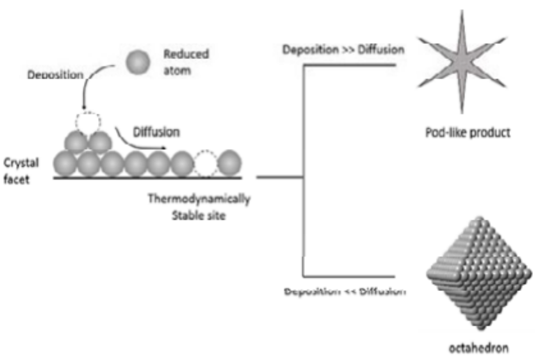

Scheme 1. Possible pathways to form pod-like and octahedral NCs.

Generally speaking, the atom deposition rate could be enhanced by increasing the ramp rate of heating whereas the diffusion rate could be promoted by improving the stirring speed. A low stirring speed and high ramp rate of heating contribute to nonhomogenous heat and mass transfer in the discussed system and could result in oversaturated atoms reduced from the precursors at a local crystal plane. In this case, the deposition would suppress the diffusion, promoting a pod-like NCs formation. When a high stirring speed and low ramp rate of heating are applied, the heat and mass transfer becomes homogeneous. An adequate and persistent diffusion thus plays a dominant role, producing the uniform octahedral NCs. In the case of high stirring speed and high ramp rate of heating, the deposition and diffusion rates may become comparable, generating polyhedron-like NCs as stated above.

To verify this, additional experiments using cubic Pt-Ni and Pt-Fe synthesis conditions were designed to examine both the discussed factors. Unlike Pt-Ni octahedral NCs. The preparation of Pt-Ni cuboid NCs involves a different nucleation and growth processes, in which the Pt nucleation initially occurs followed by the incorporation of the Ni-component. As shown in Figure 3a and 3b, a low speed of stirring (200 rpm) generated ununiform Pt-Ni pod-like NCs with branches whereas a high speed of stirring (600 rpm) yielded Pt-Ni NCs which are more closed to a cubic shape. In the case of Pt-Fe nanocube synthesis (Figure 3c and 3d), a low speed of stirring (200 rpm) and high ramp rate of heating (15 °C/min) produced pod-like NCs with branches whereas the inverse conditions (600 rpm and 5 °C/min) promoted perfect Pt-Fe cuboid NCs, which is similar to the synthesis of Pt-Ni octahedral NCs.

Based on the discussed observation, it shows consistent results with the synthetic process of Pt-Ni octahedral NCs and confirms the significant role of stirring speed and ramp rate of heating in the preparation of NCs, in which the proposed model could be used to elaborate the formation mechanism of each product.

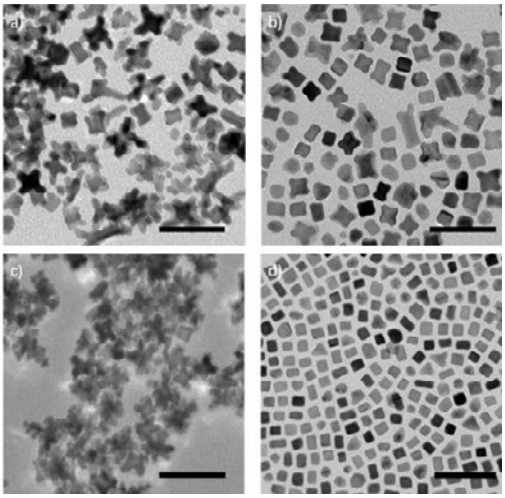

Figure 3. TEM images of a) Pt-Ni pod-like NCs from cubic synthesis (200 rpm), b) Pt-Ni cuboid NCs (600 rpm), c) Pt-Fe pod-like NCs (200 rpm, 15 °C/min), and d) Pt-Fe cuboid NCs (600 rpm, 5 °C/min). Each scale bar represents 50 nm.

CONCLUSIONS

Based on the designed syntheses of Pt-M (M = Ni, Fe) NCs, it could be confirmed that the stirring speed and ramp rate of heating do have a contribution to the morphology evolution in the growth process of an NC. The deposition and diffusion competition model could be applied for a general understanding of the correlation between the discussed experimental parameters and the resultant morphologies of the NCs. An in-depth study of these significant factors could leverage a new synthetic strategy in which essential experimental parameters are well-controlled and used to steer the direction of the designed NCs products.

ACKNOWLEDGMENTS

This work was supported by ACS PRF grant (58196-ND10), NSF (DMR-1808383), S^3IP and SUNY at Binghamton.

REFERENCES

1. C. Wang, V. Murugadoss, J. Kong, Z.F. He, X.M. Mai, Q. Shao, Y.J. Chen, L. Guo, C.T. Liu, S. Angaiah and Z.H. Guo, *Carbon* **140**, 696-733 (2018).
2. H. Du, C.X. Zhao, J. Lin, J. Guo, B. Wang, Z. Hu, Q. Shao, D. Pan, E.K. Wujcik and Z. Guo, *Chem. Rec.* **18**, 1365-1372 (2018).
3. J. Bauer, L.R. Meza, T.A. Schaedler, R. Schwaiger, X. Zheng and L. Valdevit, *Adv. Mater.* **29**, 1701850 (2017).
4. G. Song, L. Cheng, Y. Chao, K. Yang and Z. Liu, *Adv. Mater.* **29**, 1700996 (2017).
5. T.S. Rodrigues, M. Zhao, T.H. Yang, K.D. Gilroy, A.G.M. da Silva, P.H.C. Camargo and Y. Xia, *Chem. Eur. J.* **24**, 16944-16963 (2018).
6. P. Yang, J. Zheng, Y. Xu, Q. Zhang and L. Jiang, *Adv. Mater.* **28**, 10508-10517 (2016).
7. Z. Zhao, R. Misra, P. Bai, J. Gao, Y. Li, R. Guan, Z. Guo and H. Liu, *Mater. Lett.* **232**, 202-205 (2018).
8. K.D. Gilroy, X. Yang, S. Xie, M. Zhao, D. Qin and Y. Xia, *Adv. Mater.* **30**, e1706312 (2018).
9. J. Zhang and J. Fang, *J. Am. Chem. Soc.* **131**, 18543-18547 (2009).
10. Y. Luan, L. Zhang, C. Wang, J. Liu and J. Fang, *MRS Adv.*, 1-6 (2018).
11. Z. Zhao, P. Bai, R. Guan, V. Murugadoss, H. Liu, X. Wang and Z. Guo, *Mater. Sci. Eng.: A* **734**, 200-209 (2018).
12. Y. Pu, F. Cai, D. Wang, J.-X. Wang and J.-F. Chen, *Ind. Eng. Chem. Res.* **57**, 1790-1802 (2018).
13. C. Gadiyar, A. Loiudice and R. Buonsanti, *J. Phys. D: Appl. Phys.* **50** (2017).
14. Q. Liu, W. Lu, A. Ma, J. Tang, J. Lin and J. Fang, *J. Am. Chem. Soc.* **127**, 5276-5277 (2005).
15. T.R. Gordon, M. Cargnello, T. Paik, F. Mangolini, R.T. Weber, P. Fornasiero and C.B. Murray, *J. Am. Chem. Soc.* **134**, 6751-6761 (2012).
16. H. Gu, H. Zhang, J. Lin, Q. Shao, D.P. Young, L. Sun, T. Shen and Z. Guo, *Polymer* **143**, 324-330 (2018).
17. J. Chen, B. Lim, E.P. Lee and Y. Xia, *NanoToday* **4**, 81-95 (2009).
18. Y. Xia, X. Xia and H.C. Peng, *J. Am. Chem. Soc.* **137**, 7947-7966 (2015).
19. J. Zhang, H. Yang, J. Fang and S. Zou, *Nano Lett.* **10**, 638-644 (2010).